ELSEVIER

Catalysis Today 60 (2000) 73–82

CATALYSIS TODAY

www.elsevier.com/locate/cattod

Dynamics of SCR reaction over a TiO_2-supported vanadia–tungsta commercial catalyst

Isabella Nova*, Luca Lietti, Enrico Tronconi, Pio Forzatti

Dipartimento di Chimica Industriale e Ingegneria Chimica "G. Natta", Politecnico di Milano, P.zza L. Da Vinci 32, 20133 Milan, Italy

Abstract

The dynamics of NH_3 adsorption–desorption and of selective catalytic reduction (SCR) of NO with NH_3 are investigated in this work over a commercial V_2O_5–WO_3/TiO_2 catalyst by transient response techniques. Linear variations in the inlet concentration of one or more reactants are imposed while analyzing the system outlet response. The transient experiments could be successfully described by a kinetic model based on: (i) a negligible NO adsorption on the catalyst surface; (ii) a non-activated NH_3 adsorption; (iii) a Temkin-type NH_3 coverage dependence of the desorption energy; and (iv) an Eley–Rideal mechanism for the SCR reaction with a non-linear dependence of the reaction rate on the NH_3 surface coverage. The presence of low concentrations of water in the feed stream does not seem to affect the ammonia adsorption–desorption process on the surface but significantly inhibits the SCR reaction; an inhibiting effect of adsorbed NH_3 on the SCR reaction is also pointed out.

Keywords: Adsorption–desorption; Selective catalytic reduction; V_2O_5–WO_3/TiO_2 catalyst

1. Introduction

Among the different commercial technologies for NO_x abatement from power plant flue gases [1–3], the selective catalytic reduction (SCR) of NO_x by ammonia is the most widespread method. Nitrogen oxides present in the flue gases (95% NO) react with oxygen and injected ammonia according to the following reaction:

$$4NO + 4NH_3 + O_2 \rightarrow 4N_2 + 6H_2O \quad (1)$$

Commercially available catalysts are made of a TiO_2 anatase carrier supporting the active components, i.e. V_2O_5 and WO_3 (or MoO_3). Vanadia is active in the reduction of NO_x but also in the undesired oxidation of SO_2 to SO_3, and accordingly its content is kept low. WO_3 or MoO_3, which are employed in larger amounts (about 6 and 10% w/w for MoO_3 and WO_3, respectively) act as "chemical" and "structural" promoters by enlarging the temperature window of the SCR reaction and by improving the mechanical, structural and morphological properties of the catalysts [4–8].

SCR reactors are often involved in transient operation, associated, e.g. with start-up and shut-down of the plant, or with load variations. This has stimulated in the last few years a growing interest towards the study of the dynamics of the SCR reaction, which is also relevant for applications characterized by fast load changes (e.g. diesel engines or heavy trucks [9]) and for specific unsteady-state SCR processes as well (reverse-flow processes [10–13]).

Transient response methods have been extensively applied in our labs to the study of mechanistic and kinetic aspects of the SCR of NO by NH_3 [14–16] over model V_2O_5/TiO_2 and V_2O_5–WO_3/TiO_2 cata-

* Corresponding author.

0920-5861/00/$ – see front matter
PII: S0920-5861(00)00319-9

lysts; these methods consist of imposing perturbations to the reacting system (typically step changes in the inlet reactant concentration), while analyzing the outlet transient response. The features of the response are characteristic of the different steps associated with the kinetics of the reaction, and therefore dynamic information and mechanistic features of the reaction can be derived.

In this study the mechanistic and kinetic features of the SCR reaction have been addressed by a modified version of such a technique; in particular, linear variations of the inlet gas composition were performed over a commercial V_2O_5–WO_3/TiO_2 catalyst with the aim of investigating both the adsorption–desorption process of the reactants and their surface reaction as well. In principle, this different experimental procedure is more informative if compared to the usual transient response method based on step (discrete) changes in the inlet reactant concentrations: indeed the linear change of one or more reactant concentrations with a finite rate allows the analysis of the system dynamics over the full range of intermediate conditions. Eventually, quantitative kinetic indications were also obtained by analyzing the experimental results of the transient runs, based on a dynamic heterogeneous plug-flow reactor model.

2. Experimental

A commercial V_2O_5–WO_3/TiO_2 catalyst (V_2O_5= 0.62% w/w, WO_3=9% w/w) was used in this study.

The experiments were performed in a flow- microreactor system constituted by a quartz tube (6 mm i.d.) directly connected to a quadrupole mass spectrometer. The reactor was inserted into an electric furnace and the catalyst temperature was measured and controlled by means of a K-type thermocouple directly immersed in the catalyst bed. In each run 120 mg of powdered catalyst (75–100 μm) were located into the reactor; the feed gases, whose flow rates were measured and controlled by mass flow controllers, were mixed in a single stream before entering the reactor. Linear variations of the inlet reactant concentrations with time were performed by externally driving the set point values of the mass flow controllers with a Personal Computer. Care was taken in minimizing all possible dead volumes in the lines upstream and downstream of the reactor. The system was operated at atmospheric pressure and with a gas hourly space velocity of $1.4\times10^5\ h^{-1}$.

The dynamics of the ammonia and NO adsorption–desorption were investigated by means of concentration programmed adsorption–desorption (CPAD) experiments. In a typical NH_3-CPAD run, a He+2% v/v O_2 mixture was admitted to the reactor, and then the ammonia inlet concentration was varied linearly from 0 to 840 ppm at ≈32 ppm/min while keeping constant the O_2 concentration and the flow rate (rise phase). The ammonia inlet concentration was kept constant for several minutes (constant phase) and finally decreased back to zero (decrease phase).

NO CPAD experiments were performed in a similar manner, but the final NO concentration in the gases was kept at 750 ppm.

Along similar lines, the dynamics of the SCR reaction was studied by imposing linear variations of the inlet reactant concentration (CPR — concentration programmed reaction). Different types of experiments were performed: in one set (CPR of NH_3 in NO) the NO and O_2 concentrations were kept constant (750 ppm and 2% v/v, respectively) while the ammonia concentration was linearly varied from 0 to 840 ppm and then back to zero. In a second kind of experiments (CPR of NO), the ammonia and O_2 inlet concentrations were kept constant (840 ppm and 2% v/v, respectively), while the NO concentration was varied from 0 to 750 ppm and then back to 0 ppm.

CPAD and CPR experiments were performed at various temperatures, in the range 553–673 K.

3. Results and discussion

3.1. NH_3 and NO adsorption–desorption

3.1.1. NH_3-CPAD

The results of the NH_3-CPAD experiments performed at different temperatures are shown in Fig. 1 (trace a, T=613 K; trace b, T=653 K; trace c, T=673 K) along with the ammonia inlet concentration (dotted line).

In a typical run (e.g. trace a), upon increasing the inlet ammonia concentration starting at t=0 s the outlet NH_3 shows a dead time of 400 s during which no ammonia is detected in the reactor outlet stream. Then

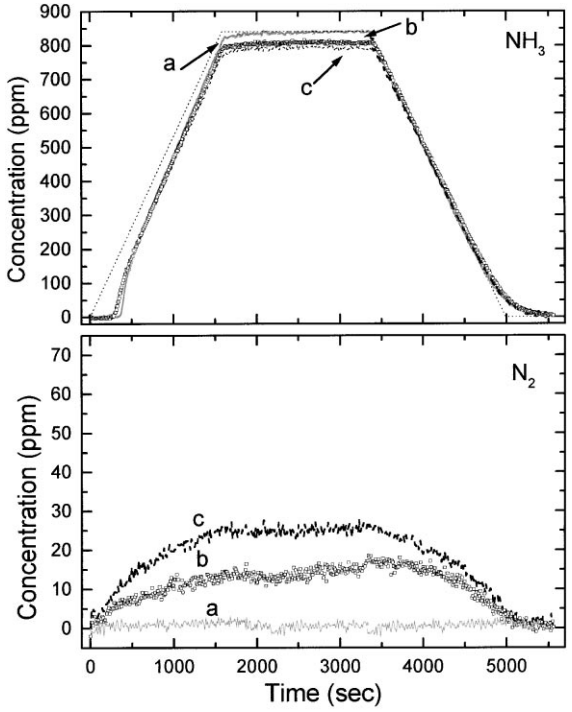

Fig. 1. Linear changes of the NH_3 inlet concentration ($0\rightarrow840\rightarrow0$ ppm) in O_2 (2%)+He over a commercial WO_3–V_2O_5/TiO_2 catalyst (V_2O_5=0.6% w/w; WO_3=9% w/w): NH_3 and N_2 concentration profiles. Dotted lines: ideal inlet NH_3 concentration; trace a: T=613 K; trace b: T=653 K; trace c: T=673 K.

the outlet NH_3 concentration rises with time, showing a knee at $t\approx450$ s. During the entire rise phase the outlet ammonia concentration is lower than the inlet one, since ammonia is adsorbed on the catalyst surface. Only during the period at constant inlet ammonia concentration (constant phase), trace a approached the inlet ammonia concentration and the system reached steady-state conditions.

During the decrease phase the ammonia inlet and outlet concentration curves remained almost superimposed for several minutes. Only at low NH_3 feed concentration, the NH_3 outlet concentration is higher than that at the inlet due to the release of adsorbed ammonia. The area between the inlet and the outlet NH_3 concentration traces in the decrease phase is smaller than that observed during the rise phase, indicating that some ammonia remains adsorbed on the catalytic surface at the end of the experiment. Heating the catalyst at high temperatures, close to 773 K, could desorb such adsorbed ammonia.

NH_3-CPAD experiments were performed in a wide temperature range (553–673 K), and similar results were always obtained. However, upon increasing the temperature the initial dead time slightly decreases in line with an exothermic adsorption phenomenon. Also, at temperatures exceeding 633 K, N_2 formation was observed, due to catalytic ammonia oxidation by oxygen. No formation of nitrogen oxides was observed at any investigated temperatures.

The effect of H_2O on the NH_3 adsorption–desorption process was also investigated, by performing experiments in the presence of 0.8% v/v H_2O in the feed flow. In spite of the fact that the H_2O content is nearly one order of magnitude higher than that of NH_3, no significant changes in the NH_3 adsorption–desorption characteristics were observed at any investigated temperature. Indeed the outlet ammonia concentration traces measured in the experiments performed in the absence and in the presence of water are almost superimposed, during both the rise and the decrease phases. This suggests that for the investigated water concentration levels the competition between ammonia and water for the adsorption on the acid catalyst sites is not appreciable.

CPAD experiments with NO instead of ammonia were also performed at different temperatures in order to study the NO adsorption characteristics on the catalyst surface. In all cases the outlet NO concentration profiles closely resemble those of the inlet concentration, thus indicating that NO does not appreciably adsorb onto the catalyst, as reported by several authors [14,17,18]. Accordingly the CPAD data are in line with the hypothesis indicating that the SCR reaction occurs between a strongly adsorbed NH_3 species and a gas-phase or weakly adsorbed NO molecule, according to an Eley–Rideal mechanism [14,18].

3.2. SCR of NO by NH_3

3.2.1. CPR of NH_3 in NO

Fig. 2 displays the results of the NH_3-CPR experiments performed at different temperatures (trace a, T=553 K; trace b, T=613 K; trace c, T=673 K). The results are shown in terms of ammonia, nitrogen oxide and nitrogen outlet concentration with time; the

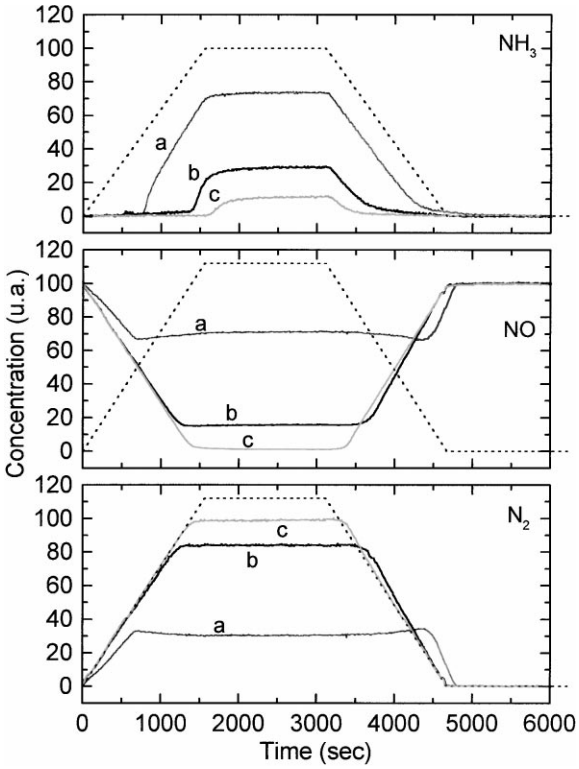

Fig. 2. Linear changes of the NH_3 inlet concentration (0→840→0 ppm) in NO (750 ppm)+O_2 (2%)+He: NH_3, NO and N_2 concentration profiles. Dotted line: ideal inlet NH_3 concentration; trace a: T=553 K; trace b: T=613 K; trace c: T=673 K.

ammonia inlet concentration profile is also reported (dotted lines).

In the run performed at T=553 K (trace a), during the rise phase the ammonia outlet concentration shows a long dead time (≈800 s) followed by a rapid increase. Eventually the ammonia concentration approaches a steady-state value, which is lower than the inlet ammonia concentration, as ammonia is consumed by the SCR reaction. On the other hand, no dead time is observed in the ammonia outlet concentration during the decrease phase. There is no ammonia left on the catalyst surface at the end of the experiment as revealed by subsequent heating of the catalyst. This indicates that ammonia is completely consumed by gaseous NO.

A different dynamic behavior is associated with NO. Indeed NO is consumed as soon as ammonia is fed to the reactor, it shows a weak minimum near 700 s and then it slightly increases up to the end of the NH_3 rise phase (t=1500 s). During the ammonia decrease phase, the NO concentration remains constant for several minutes, it shows a minimum near 4400 s and then slowly increases up to the inlet value.

The evolution with time of N_2 and H_2O (this latter not reported in the figure) is symmetrical to that of NO. No formation of other species (e.g. N_2O) was observed, thus indicating the occurrence of a genuine SCR process.

The different NH_3 and NO dynamics observed during the NH_3 rise phase is in line with a mechanism that involves adsorbed NH_3 and gaseous NO. A very fast NH_3 adsorption process should be considered to explain the immediate NO consumption in correspondence of the NH_3 admission to the reactor. Also, the observation that the NO consumption is not affected at high NH_3 inlet concentration during both the increase and decrease phase suggests a complex dependence of the NO consumption rate on the ammonia concentration. Notably, NO is still consumed after the end of the experiment, near 4600 s, when both the inlet and outlet NH_3 concentration is nil. This points out to the existence of a "reservoir" of ammonia-adsorbed species, which is involved in the reaction once the ammonia gas-phase concentration is reduced. These results have already been underlined analyzing experiments run by performing step changes in the reactants feed flow [14].

To better analyze such aspects, the outlet ammonia, NO and nitrogen concentrations measured at 553 K are represented in Fig. 3 as a function of the inlet ammonia concentration. Dotted lines in the figure represent the inlet concentration, whereas traces a and b show the NH_3, NO and N_2 concentrations measured during the inlet ammonia concentration increase and decrease phases, respectively. A hysteresis cycle clearly appears for the three species, related to the fact that during the NH_3 decrease phase the amount of ammonia adsorbed onto the catalyst surface is higher if compared to that present in correspondence of the rise phase. These data again suggest that ammonia adsorption is faster compared to desorption. Also, it clearly points out the presence of the ammonia "reservoir", since appreciable NO consumption is measured at $C_{NH_3} = 0$ during the decrease phase.

Inspection of Figs. 2 and 3 points out other interesting features, i.e. the presence of a weak minimum in the NO concentration (which in Fig. 3

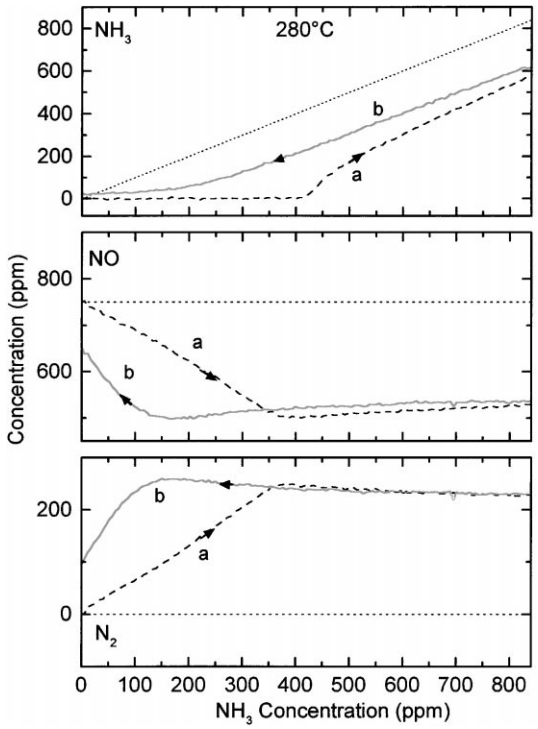

Fig. 3. Linear changes of the NH_3 inlet concentration in $NO+O_2$: NH_3, NO and N_2 outlet concentration as a function of NH_3 inlet concentration at 553 K. Dotted lines: inlet concentrations; dashed lines: outlet concentration during the rise phase; solid lines: outlet concentrations during the decreasing phase.

appears at $C_{NH_3} = 370$ and 170 ppm during the rise and the decrease phase, respectively), followed by a decrease of the NO consumption at higher ammonia inlet concentration. This feature, accompanied by a symmetrical N_2 evolution, may be associated with a weak-inhibiting effect on the SCR reaction of excess ammonia adsorbed on the catalyst surface. In line with the presence of a "reservoir" of adsorbed ammonia, the minimum in the NO concentration appears at lower inlet NH_3 concentration during the decrease phase. It is however noteworthy that the ammonia inhibiting effect is not associated with a transient phenomenon, since it was also confirmed by steady-state experiments performed with different concentrations of ammonia in the feed stream.

NH_3-CPR experiments have also been performed at higher temperatures, and Fig. 2 shows the results obtained at 613 and 673 K (traces b and c, respectively). On increasing the reaction temperature, from Fig. 2 it is observed that: (i) the initial dead time in the NH_3 concentration increases; (ii) the steady-state concentrations of ammonia and NO are lower; (iii) the inhibiting effect of ammonia on the NO conversion progressively disappear. Also, by increasing the temperature, the hysteresis cycle reduces, so that transient data are almost superimposed to steady-state results. Such effects are in line with the increased rate of both the ammonia adsorption–desorption processes and SCR surface reaction as well, leading to a reduction of the ammonia coverage (and storage) on the catalyst surface.

The effect of the addition of water vapor (0.8 and 5% v/v) to the feed stream on the dynamics of the SCR reaction was also investigated. Fig. 4 compares the NO and nitrogen profiles obtained upon performing NH_3-CPR experiments at T=613 K in the absence of water (trace a) and in presence of 0.8 and 5% v/v of

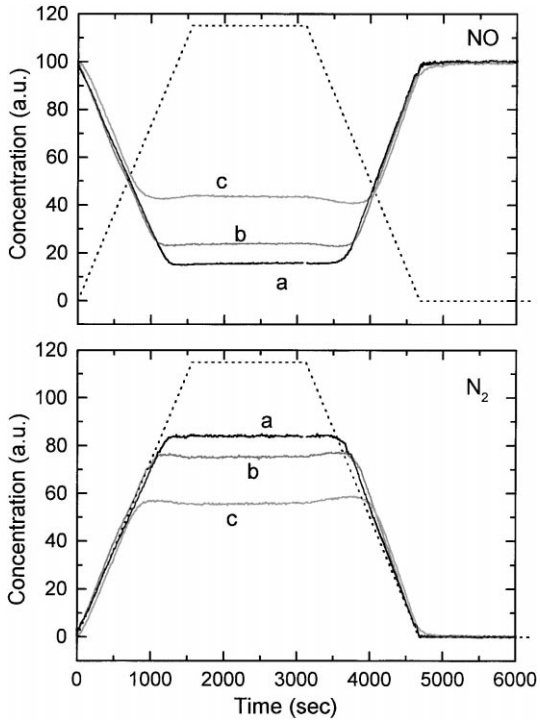

Fig. 4. Linear changes at T=613 K of the NH_3 inlet concentration ($0\rightarrow840\rightarrow0$ ppm) in NO (750 ppm)+H_2O+O_2 (2%)+He: NO and N_2 concentration profiles. Dotted lines: ideal inlet NH_3 concentration; trace a: H_2O=0%; trace b: H_2O=0.8%; trace c: H_2O=5%.

water (traces b and c, respectively). Dotted lines in Fig. 4 represent the ammonia inlet concentration curves.

From Fig. 4 it appears that the presence of water does not apparently modify the dynamics of the SCR reaction, but it does affect the reactivity of the catalysts. On increasing the water content a decrease in the NO steady-state values is observed in line with the well-known inhibiting effect of water on the SCR reaction [19,20]. Considering that as observed above, the presence of water (0.8% v/v) does not appreciably modify the adsorption–desorption characteristics of NH_3, it is speculated that a simple competition effect of H_2O on the NH_3 adsorption on the catalyst surface cannot completely account for the inhibiting effect of water on the SCR reaction.

3.2.2. CPR of NO in NH_3

Experiments were also performed in which the NO inlet concentration is varied linearly (0→750→0 ppm) keeping NH_3 concentration constant (840 ppm)+O_2 (2% in He). Selected results obtained at different temperatures are shown in Fig. 5, in terms of ammonia, nitrogen oxide and nitrogen outlet concentrations as a function of time (trace a, T=553 K; trace b, T=613 K; trace c, T=673 K). The NO inlet concentration profile is also reported in Fig. 5 as dotted lines.

In a typical run (e.g. trace a, T=553 K) the NH_3, NO and N_2 outlet concentrations exhibit very different dynamic behavior if compared to that obtained in the ammonia CPR experiments and reported in Fig. 2. As a matter of fact, the ammonia consumption and the corresponding N_2 production is evident as soon as NO is fed to the reactor without showing any dead time. If the outlet concentrations of the different species are plotted as a function of the inlet NO concentration as already done for the NH_3-CPR experiments (Fig. 3), no hysteresis cycle can be observed: accordingly, the data seems to indicate the lack of any reservoir of NO-related species onto the catalyst surface. Hence these results confirm that NO as opposite to ammonia is not involved in adsorption–desorption processes on the catalyst surface, and provide another piece of evidence that the SCR reaction occurs between a strongly adsorbed NH_3 species and a gas-phase or weakly adsorbed NO molecule.

Results similar to those discussed above have been obtained at other temperatures, i.e. 613 and 673 K

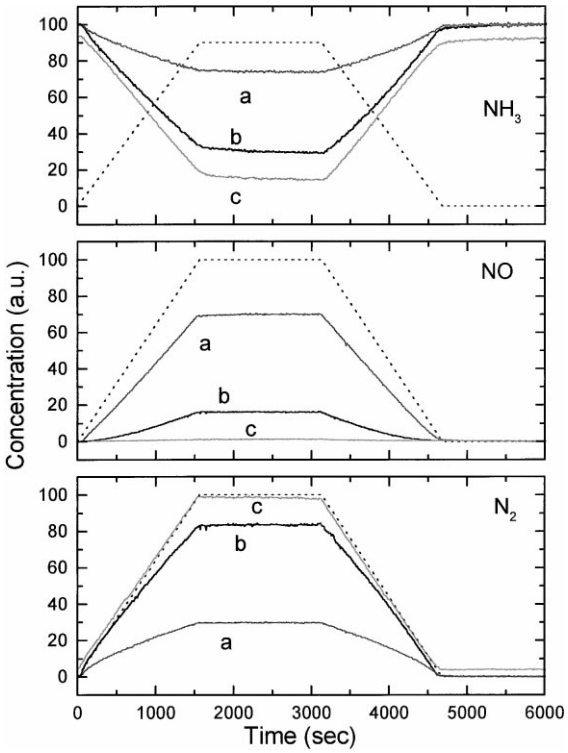

Fig. 5. Linear changes of the NO inlet concentration (0→750→0 ppm) in NH_3 (840 ppm)+O_2 (2%)+He: NH_3, NO and N_2 concentration profiles. Dotted lines: ideal inlet NO concentration; trace a: T=553 K; trace b: T=613 K; trace c: T=673 K.

(traces b and c, respectively). However, from Fig. 5 it appears that on increasing the reactor temperature an increase in the catalyst reactivity is observed leading to a lower NH_3 and NO steady-state concentration values, and correspondingly high N_2 production. Notably, in the experiment performed at 673 K (trace c), the outlet ammonia concentration in the absence of NO is slightly below the inlet concentration value (840 ppm) due to the occurrence of the ammonia oxidation reaction to N_2 as already pointed out by the NH_3-CPAD experiments previously reported (see Fig. 1).

3.3. Kinetic analysis of transient experiments

A dynamic one-dimensional heterogeneous PFR model of the microreactor, already developed to describe the step addition experiments reported in [14] is used here to analyze the bulk set of data obtained

by imposing linear variations in the inlet reactant concentrations, some of which are displayed in Figs. 1–5. The model, which neglects the presence of both intraparticle catalyst gradients and external mass transfer limitations (as verified on the basis of theoretical diagnostic criteria [21,22]) is based on the NH_3 mass balance on the catalyst surface, Eq. (2), and on the NH_3, NO and N_2 mass balances in the gas stream, Eqs. (3)–(5), respectively [14]:

$$\frac{\partial \theta_{NH_3}}{\partial t} = r_a - r_d - r_{NO} - r_{ox} \quad (2)$$

$$\frac{\partial C_{NH_3}}{\partial t} = -v\frac{\partial C_{NH_3}}{\partial z} + \Omega_{NH_3}(r_a - r_d - r_{NO} - r_{ox}) \quad (3)$$

$$\frac{\partial C_{NO}}{\partial t} = -v\frac{\partial C_{NO}}{\partial z} + \Omega_{NH_3} r_{NO} \quad (4)$$

$$\frac{\partial C_{N_2}}{\partial t} = -v\frac{\partial C_{N_2}}{\partial z} - \Omega_{NH_3}(r_{NO} + 0.5 r_{ox}) \quad (5)$$

where the symbols are defined in Section 5. Notably, as opposite to the model developed in [14], the ammonia oxidation reaction (r_{ox}) has also been included in this case.

The following rate expressions were used for NH_3 adsorption and desorption from the catalyst surface:

$$r_a = k_a^0 \exp\left(-\frac{E_a}{RT}\right) C_{NH_3}(1 - \theta_{NH_3}) \quad (6)$$

$$r_d = k_d^0 \exp\left(-\frac{E_d}{RT}\right) \theta_{NH_3} \quad (7)$$

where k_a^0 and k_d^0 are the pre-exponential factors of the rate constant for NH_3 adsorption and desorption, respectively, E_d the activation energy for NH_3 desorption, and θ_{NH_3} the NH_3 surface coverage. As evident from Eq. (7), on the basis of previous indications [14] a non-activated ammonia adsorption process has been considered. On the other hand, different rate expressions were used for NH_3 desorption: a simple Langmuir approach, that considers a constant value of the desorption activation energy E_d, and a Temkin-type coverage dependence of the desorption energies ($E_d = E_d^0(1 - \alpha\theta_{NH_3})$), which takes into account the catalyst surface heterogeneity in agreement with the physico-chemical characterization of the catalysts [24–27].

The following rate expressions were used for NH_3 oxidation and SCR reaction, respectively:

$$r_{ox} = k_{ox}\theta_{NH_3} \quad (8)$$

$$r_{NO} = k_{NO} C_{NO} \theta^*_{NH_3} \left(1 - \exp\left(-\frac{\theta_{NH_3}}{\theta^*_{NH_3}}\right)\right) \quad (9)$$

From Eq. (9) it appears that r_{NO} is essentially independent of the ammonia surface coverage above a critical NH_3 surface concentration ($\theta^*_{NH_3}$). This empirical rate expression accounts for the complex dependence of the rate of NO consumption on the NH_3 surface coverage, but not for the observed weak-inhibiting effect of NH_3 on the SCR reaction. Notably, the ammonia inhibiting effect on the SCR reaction could only be pointed out in this study having imposed a linear variation in the inlet ammonia concentration.

The data fit was performed by using the experimental data obtained in the study of the NH_3 adsorption–desorption process at different temperatures (NH_3-CPAD experiments, Fig. 1) and the results of the experiments in which the inlet NH_3 concentration was changed in flowing NO+O_2 (NH_3-CPR experiments, Fig. 2).

Fig. 6 shows a typical fit of the data obtained in the case of the NH_3-CPR experiment performed at T=553 K already shown in Fig. 2 (symbols: experimental data; solid line: model fit). From Fig. 6 it clearly appears that a satisfactory data fit could be obtained for the ammonia CPR experiment performed at 553 K, since the model was able to reproduce all the major features of the CPR results. Only the observed weak-inhibiting effect of ammonia on the SCR reaction was not accounted for by the model, which indeed does not include any inhibition term in the rate equations. This point deserves further investigation and work is currently in progress in our labs to arrive at a better analysis of the observed ammonia inhibition effect. The soundness of the model is also demonstrated by the fact that it does adequately describe the results of experiments in which both linear and step changes have been applied, and over both home-made and commercial catalyst samples.

Besides the data shown in Fig. 6 an excellent fit of the experimental data was also obtained at the other investigated temperatures and in the case of the NH_3-CPAD runs as well. Notably, in the case of

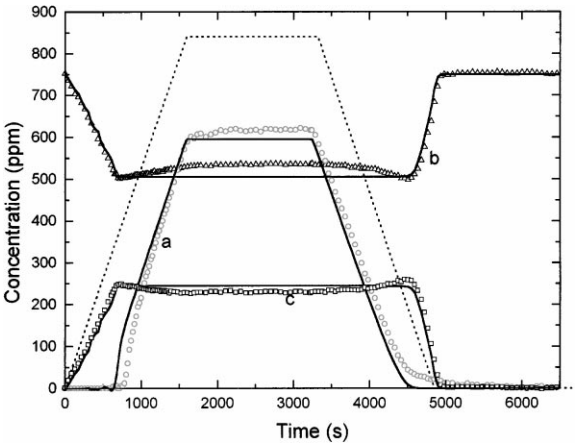

Fig. 6. Linear changes of the NH_3 inlet concentration ($0\rightarrow840\rightarrow0$ ppm, dotted line) in O_2 (2%)+He (trace a) and in NO (750 ppm)+O_2 (2%)+He: NH_3 (trace b) and NO (trace c) concentration profiles. Symbols: experimental data; solid lines: model fit (k_a^0=33.87 m^3/mol s, k_d^0=2.2E+6 s^{-1}, E_d^0=23.0 kcal/mol, γ=0.256, Ω_{NH_3}=270 m^3/mol, k_{ox}^0=3.25E+6 s^{-1}, E_{ox}^0=28.8 kcal/mol, $k_{NO}^0=1.18\times10^8$ s^{-1}, E_{NO}^0=19.2 kcal/mol, $\theta^*_{NH_3}$=0.06).

the ammonia adsorption–desorption studies, it was found that a simple Langmuir approach could not adequately represent the experimental data, whereas a satisfactory data fit was obtained by using a more complex Temkin-type desorption process, which consider a linear variation of the energy of ammonia desorption with coverage. This datum is however in line with the results of the chemico-physical characterization of the samples, suggesting the presence of acid sites of different strengths, indicative of surface heterogeneity [23–28].

In Fig. 6 the estimates of the kinetic parameters used to fit the experimental data are reported: a NH_3 desorption activation energy at zero-coverage of 23 kcal/mol and SCR reaction activation energy of 19 kcal/mol have been calculated. These values are in line with literature indications for vanadia-based catalysts [29,30]. Higher values of the activation energy for the ammonia oxidation reaction have been estimated near 29 kcal/mol. It is worth emphasizing that essentially the same set of kinetic parameters could be obtained either by superimposing the kinetics of the SCR reaction to the NH_3 adsorption–desorption kinetics independently determined from the ammonia CPAD experiments (Fig. 1) or by simultaneous analysis of the CPAD and CPSR data. This confirms the adequacy of the adopted model for the description of the transient adsorption–desorption and reaction kinetics as well as the virtual superposition of the two processes. The soundness of the kinetic model is further confirmed by the analysis of the NO CPSR experiments, which could be nicely described on a purely predictive basis by using the kinetic parameter estimates reported in Fig. 6. Work is currently in progress to analyze quantitatively the effect of water addition on adsorption/desorption of ammonia and on the reactivity in the SCR reaction.

4. Conclusions

This work demonstrated the potentiality of the CPAD/CPSR transient technique in evaluating kinetic and mechanistic aspects of the SCR process. The adsorption–desorption process of the reactants was investigated independently from their surface reaction, thus allowing separate investigation of the sequence of steps of the reaction. The major results derived from this study can be summarized as follows:

1. NH_3 is strongly adsorbed on the V_2O_5–WO_3/TiO_2 commercial catalyst sample. Surface heterogeneity must be considered to describe the kinetics of NH_3 adsorption–desorption: a non-activated NH_3 adsorption process and a Temkin-type coverage dependence of the desorption energy is well suited to represent the dynamic data with values of the activation energy for ammonia desorption at zero-coverage of 26 kcal/mol. As opposite to NH_3, NO does not adsorb appreciably on the catalyst surface. This is in line with a reaction mechanism involving a gas-phase or weakly adsorbed NO and a strongly adsorbed ammonia species, according to an Eley–Rideal pathway.
2. Reactivity data indicated that the rate of the deNO_x reaction is virtually independent of the ammonia surface concentration for NH_3 coverage above a characteristic “critical” value. Also, it was found that ammonia is stored on the catalyst surface, and is available for the reaction once the NH_3 gas-phase concentration is decreased.
3. The transient behavior of the SCR reaction upon linear changes of the NH_3 or NO inlet concentrations is in line with an Eley–Rideal pathway

involving a strongly adsorbed species (NH_3) and a gaseous or weakly adsorbed species (NO); the observed dynamic behavior of the SCR reaction could be nicely fitted according to a one-dimensional heterogeneous unsteady PFR model, superimposing the NH_3 adsorption–desorption process, with kinetics obtained by the independent ammonia adsorption study, to the SCR reaction.

4. The presence of low concentration of water in the feed stream does not seem to affect the ammonia adsorption–desorption process on the surface acid sites at any surface coverage, but it significantly inhibits the SCR reaction; an inhibiting effect of adsorbed NH_3 on the SCR reaction has also been pointed out.

5. Nomenclature

C_i	gas-phase concentration of species i (mol/m^3_{gas})
E_a	activation energy for NH_3 adsorption (kcal/mol)
E_d	activation energy for NH_3 desorption (kcal/mol)
E^0_d	activation energy for NH_3 desorption at zero-coverage (kcal/mol)
E_{NO}	activation energy for the $deNO_x$ reaction (kcal/mol)
k^0_a	pre-exponential factor for NH_3 adsorption rate constant ($m^3/mol\,s$)
k_a	rate constant for NH_3 adsorption ($m^3_{gas}/(m^3_{cat}\,s)$)
k^0_d	pre-exponential factor for NH_3 desorption rate constant (s^{-1})
k_d	rate constant for NH_3 desorption ($mol/(m^3_{cat}\,s)$)
k_{ox}	rate constant for ammonia oxidation (s^{-1})
k^0_{NO}	pre-exponential factor for the $deNO_x$ reaction rate constant ($m^3/mol\,s$)
k_{NO}	kinetic constant for the $deNO_x$ reaction rate constant ($m^3/mol\,s$)
r_a	rate of NH_3 adsorption (s^{-1})
r_d	rate of desorption (s^{-1})
r_{NO}	rate of NO consumption (s^{-1})
r_{ox}	rate of ammonia oxidation (s^{-1})
t	time (s)
v	gas linear velocity (m/s)
z	reactor or monolith axial coordinate

Greeks

α	NH_3/NO molar feed ratio
ε	void fraction
γ	parameter for the surface coverage dependence
θ_i	surface coverage of species i
$\theta^*_{NH_3}$	parameter for the NH_3 surface coverage dependence
Ω_{NH_3}	catalyst NH_3 adsorption capacity (mol/m^3_{cat})

References

[1] H. Bosch, F.J.J. Janssen, Catal. Today 2 (1988) 369.
[2] F. Nakajima, I. Hamada, Catal. Today 29 (1996) 109.
[3] P. Forzatti, L. Lietti, Heter. Chem. Rev. 3 (1996) 33.
[4] S. Matsuda, T. Kamo, A. Kato, F. Nakajima, Ind. Eng. Chem. Res. 21 (1982) 48.
[5] J.P. Chen, R.T. Yang, Appl. Catal. A 80 (1992) 135.
[6] L. Lietti, P. Forzatti, F. Bregani, Ind. Eng. Chem. Res. 35 (11) (1996) 3884.
[7] L. Alemany, L. Lietti, N. Ferlazzo, P. Forzatti, G. Busca, E. Giamello, F. Bregani, J. Catal. 155 (1995) 117.
[8] L. Casagrande, L. Lietti, I. Nova, P. Forzatti, A. Baiker, Appl. Catal. B 17 (1998) 245–258.
[9] L. Andersson, P.L.T. Gabrielsson, C.U.I. Odenbrand, AIChE J. 40 (11) (1994) 1911.
[10] D. Agar, W. Ruppel, Chem. Eng. Sci. 43 (1988) 2073.
[11] L.N. Bobrova, A.S. Noskov, Y.S. Matros, Catal. Today 17 (1993) 293.
[12] K. Hedden, R. Ramanda Rao, N. Schon, Chem. Ing. Technol. 65 (1993) 1506.
[13] Noskov, L. Bobrova, G. Bunimovich, O. Goldman, A. Zagoruiko, Y. Matros, Catal. Today 27 (1996) 315.
[14] L. Lietti, I. Nova, S. Camurri, E. Tronconi, P. Forzatti, AIChE J. 43 (1997) 2559.
[15] L. Lietti, I. Nova, E. Tronconi, P. Forzatti, Catal. Today 45 (1998) 85.
[16] P. Forzatti, L. Lietti, I. Nova, E. Tronconi, in: Chemical Engineering Greetings to Prof. Mario Dente, Ed. AIDIC, Italian Association of Chemical Engineering, Milan, Italy, 1999.
[17] T.Z. Srnak, J.A. Dumesic, B.S. Clausen, E. Törnqvist, N.Y. Topsøe, J. Catal. 135 (1992) 246.
[18] N.-Y. Topsoe, J.A. Dumesic, H. Topsoe, J. Catal. 151 (1995) 241.
[19] G. Ramis, C. Cristiani, P. Forzatti, G. Busca, J. Catal. 124 (1990) 574.
[20] S.A. Selim, Ch.A. Philip, R. Mikhail, Sh. Thermochim. Acta 36 (1980) 287.
[21] D.E. Mears, Ind. Eng. Chem. Process. Des. Dev. 10 (4) (1971) 541.

[22] G. Froment, K. Bischoff, Chemical Reactor Analysis and Design, Wiley, New York, 1979.
[23] N.-Y. Topsøe, J. Catal. 128 (1991) 499.
[24] G. Ramis, G. Busca, P. Forzatti, C. Cristiani, L. Lietti, F. Bregani, Langmuir 8 (1992) 1744.
[25] L. Lietti, P. Forzatti, G. Ramis, G. Busca, F. Bregani, Appl. Catal. B 3 (1993) 13.
[26] G. Ramis, G. Busca, F. Bregani, P. Forzatti, Appl. Catal. 64 (1990) 259.
[27] G. Ramis, G. Busca, F. Bregani, P. Forzatti, Catal. Sci. Technol. 1 (1991) 189.
[28] H. Schneider, S. Tschudin, M. Schneider, A. Wokaun, A. Baiker, J. Catal. 147 (1994) 5.
[29] W.C. Wong, K. Nobe, Ind. Eng. Chem. Prod. Res. Dev. 23 (1984) 564.
[30] V.I. Marshneva, E.M. Slavinskaya, O.V. Kalinkina, G.V. Odegova, E.M. Moroz, G.V. Lavrova, A.N. Salanov, J. Catal. 155 (1995) 171.